S100P-Induced Cell Migration and Metastasis

The presence of S100P protein in cancer cells is strongly associated with reduced survival times of patients suffering from a number of cancers. It has been shown previously that S100P is a potent inducer of metastasis in a model system and it is likely that this metastasis-inducing ability underlies its association with reduced patient survival. However, the molecular mechanisms involved in S100P-driven metastasis are only now beginning to be elucidated and the evidence points to S100P enhancing cell migration and cell invasion. It is now shown that in the same cell system S100P enhances cell migration by two separate mechanisms. One pathway being intracellular, involves changes in the numbers of focal adhesions. The second pathway occurs at the cell membrane and does not involve changes in the number of focal adhesions, but involves extracellular/membrane bound S100P and is inhibited by specific inhibitors of plasmin. Importantly, mutation of the C-terminal amino acid of S100P, not only abolishes both pathways, but also markedly reduces the metastasis-inducing ability of S100P, thus identifying a possible target for the reduction of S100P-induced metastasis.

1. Introduction

Elevated levels of some EF-hand-containing, calcium-binding members of the S100 family of proteins are associated with the development of many human cancers [1][2]. Increased immunohistochemical levels of S100P are associated with markedly reduced survival times of patients with breast [3][4], hepatocellular [5], early stage non-small cell lung [6], colon [7][8], and ovarian [9][10] cancers. The associations of S100P with reduced patient survival times are likely to arise from the ability of S100P to induce a metastatic phenotype [3]. However, the molecular pathways by which S100P exerts its metastasis-inducing potential are not yet fully understood [2].

The crystal structure of calcium-bound S100P protein shows that it is a homodimer with each 95-amino-acid monomer displaying the four α-helical structures common to most other S100 proteins [11]. Helix 4 of each monomer ends at amino acid 92, leaving a short, three-amino acid, presumably unstructured sequence, GLK, at the C-terminus [11]. In the apo-form, the presumably unstructured C-terminal region was found to be six amino acid residues longer, KYFEKAGLK, using Nuclear Magnetic Resonance techniques [12]. C-terminal regions of other S100 proteins, for example, S100A4 [13], have been reported to be unstructured and dynamic.

S100 proteins act by interacting with extracellular and intracellular protein targets [14]. Thus, extracellular S100P can interact with the cell-membrane-located RAGE receptor, thereby activating intracellular signalling pathways [15] and with the extracellular plasminogen activator, tPA, to enhance plasmin-dependent cell invasion [16], but its relationship to metastasis is unknown. Intracellular S100P can also interact with cytoskeletal proteins, ezrin [17], IQGAP1 [18], and non-muscle myosin II isoforms A (NMMIIA) and C (NMMIIC) [19], all with high nM range affinities [17][18][19], often causing increased cell migration [19][20]. In the case of NMMIIA, it has been shown using Fluorescence Lifetime Imaging that S100P can interact with NMMIIA in living cells [19]. In cells in which NMMIIA had been knocked down using siRNA, S100P induction lost its effect on cell migration [19]. Furthermore, in an inducible system, expression of S100P led directly to redistribution of NMMIIA filaments and their dissociation. In a cell-free system, S100P can partially dissociate myosin IIA filaments [19]. These observations taken together show that S100P can interact with myosin IIA in vivo and, through dissociation of the NMMIIA filaments, can affect cell migration. It has been shown previously that deletion of the C-terminal lysines of the related metastasis-inducing protein, S100A4, abrogates its metastasis-inducing potential [21][22] in a well-characterised rat model system of human breast cancer metastasis [3][23][24][25].

2. The Effect of C-Terminal Mutants of S100P on Tumorigenesis and Metastasis

The benign rat mammary tumour-derived cell line, Rama 37, has a long track record of testing for the metastatic potential of experimentally-expressed genes and proteins when injected into the mammary fat pads of immunocompetent

syngeneic rats [3][23][25][26][27]. Genes and proteins, including S100P, which confer a metastatic phenotype upon the benign Rama 37 cells in this system, have subsequently been shown to be associated also with reduced patient survival time when they are found in the cancer cells of human patients [3][28][29][30]. Transfected Rama 37 cell clones and pools expressing wild-type S100P, the K95A, or ΔK95 mutant S100P proteins exhibited similar incidences of mammary tumour formation (**Table 1**). Thus, the C-terminal mutants did not affect the tumorigenicity of the cells. Cells expressing wild-type S100P exhibited high incidences of metastasis, with 70% (cell clone) and 75% (cell pool) of tumour-bearing rats exhibiting lung metastases (**Table 1**), similar to those reported previously [3]. Examples of immunocytochemical staining of the tumours and metastases arising from injection into the mammary fat pads of syngeneic rats of Rama 37 cells expressing wild-type S100P have been published previously [3]. The cell clone and pool expressing K95A mutant S100P protein exhibited incidences of metastasis of 33% and 47%, which were lower than those of the wild-type clone and pool (**Table 1**). The transfected cell clones and pools expressing ΔK95 mutant S100P protein exhibited incidences of metastasis (clone 16%, pool 11%), which were lower than wild-type S100P-expressing clone and pool (**Table 1**). Overall, mutation/removal of the C-terminal amino acid of S100P significantly reduces its ability to cause metastasis in a rodent model system in vivo.

Table 1. Incidences of tumours and metastases.

Transfected DNA (Designation of Cell Line) [a]	Incidence of Mammary Tumours (%) [b]	p-Value [c]	Incidence of Metastasis (%) [d]	p-Value [e]
None. Untransfected [f]	18/20 (90)		0/18	
Rama 37 Vector only [f]				
Clone	19/20 (95)		0/19 (0)	
Pool	23/23 (100)		2/23 (9)	
S100P wild-type				
Clone	27/27 (100)		19/27 (70)	
Pool	20/20 (100)		15/20 (75)	
K95A S100P				
Clone	21/21 (100)	p > 0.9999	7/21 (33)	p = 0.019
Pool	19/19 (100)	p > 0.9999	9/19 (47)	p = 0.105
ΔK95 S100P				
Clone	19/19 (100)	p > 0.9999	3/19 (16)	p = 0.0003
Pool	19/21 (90)	p > 0.9999	2/19 (11)	p < 0.0001

[a] *Nomenclature—S100P wild type, cells expressing non-mutant S100P protein; K95A S100P, cells expressing S100P with C-terminal lysine changed to alanine; ΔK95 S100P, cells expressing S100P with C-terminal lysine deleted; clone, a cell line derived from a single colony of transfected cells; pool, an uncloned pool of transfected cells; experimental unit, clone or pool of transfected cells.* [b] *Number of tumours/number of animals inoculated. Animals were randomised before use to ensure individual observations were independent for statistical analysis, encrypted, and hence blinded to the recorder of macroscopic and histological results to avoid bias. No adverse effects reported.* [c] *p-values by standard 2-sided Fisher's Exact test for tumour incidences in vivo of a clone or a pool of transfected cells expressing K95A or ΔK95 mutant S100P proteins compared with a clone or a pool of transfectant cells expressing wild-type S100P protein.* [d] *Numbers of animals (%) with lung metastases/numbers of animals with tumours.* [e] *p-values by standard 2-sided Fisher's Exact test for incidences of metastasis in vivo of a clone or a pool of transfected cells expressing K95A or ΔK95 mutant S100P proteins compared with a clone or a pool of transfectant cells expressing wild-type S100P protein.* [f] *For purpose of comparison only, the results for Rama 37 cells and vector are taken from Ismail, T. et al. [31], with permission of Oxford University Press.*

3. S100P Mutants and Altered Cytoskeletal Organisation

Wild-type rS100P protein bound to rNMMIIA in vitro with a Kd of 370–470 nM, consistent with previously published values of 430–500 nM [19]. The K95A and ΔK95 mutant rS100P proteins exhibited 6 to 13-fold reduced affinity for immobilised rNMMIIA (equilibrium Kd, 2.3 µM and 2.7 µM; kinetic Kd, 4.1 µM and 6 µM, respectively) than the wild-type protein, mainly due to an 8 to 13-fold increased rate of dissociation. The observation that the association rate of S100P with NMMIIA in vitro was not affected by the C-terminal mutations but that the dissociation rate was suggests that the C-terminal lysine might be required not for initial binding but for structural stability of the complex.

Immunofluorescence staining of fixed, control, S100P-negative Rama 37 cells revealed cytoplasmic localisation of NMMIIA filamental structures along the edges of the cells (**Figure 1**a). In cells expressing wild-type S100P, there was a 20.5-fold reduction in the proportion of cells exhibiting this control cell distribution of NMMIIA ($p < 0.0001$). Whilst there was some background, possibly non-specific, staining for S100P in the S100P-negative cells (**Figure 1**b and Figure 3B) that was not observed in Western blots (Figure 3A below and Clarke et al. [16]), cells expressing wild-type S100P protein exhibited markedly stronger staining with intense foci of S100P in the cytoplasm and nuclear regions of the cells (**Figure 1**e). There were extensive clusters of NMMIIA foci, mainly at the cell periphery (**Figure 1**d), with only some colocalising with S100P, predominantly in the perinuclear region of the cells (**Figure 1**f). The foci of S100P staining in the wild-type-S100P-expressing Rama 37 cells observed here is similar to that observed previously in MCF-7 cells [19] using a glass substratum; in contrast, in the present experiments, the cells were grown on a fibronectin substratum. Thus, the punctate staining pattern has been observed in two different cell systems, grown on two different substrata. However, the strong nuclear staining observed in the MCF-7 cells was not seen in the present experiments. The structural basis of the punctate staining of wild-type S100P and how it might enhance cell migration in the MCF-7 cells [19] and in Rama 37 cells in the present experiments is unknown.
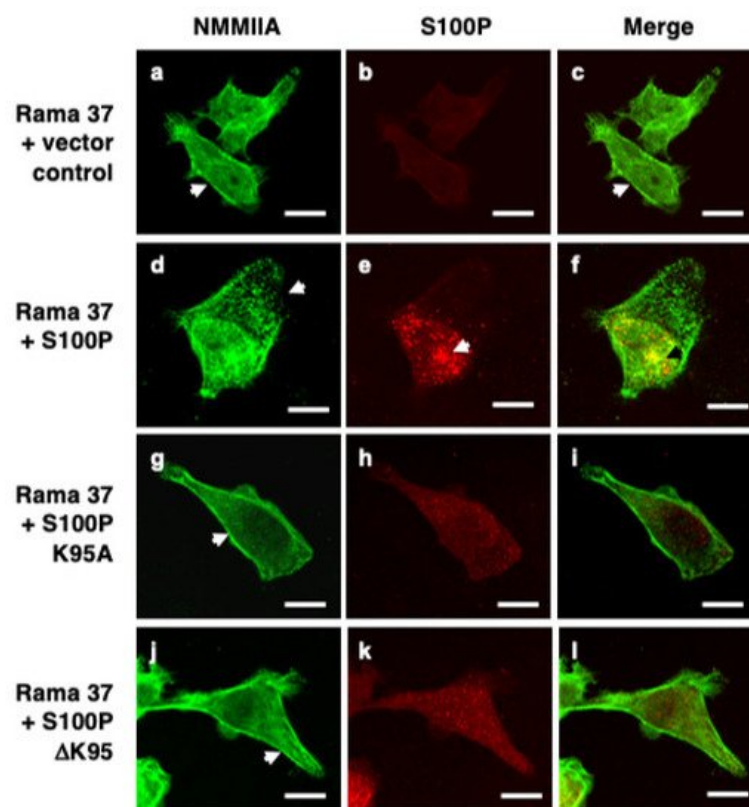

Figure 1. Immunofluorescence localisation of NMMIIA and S100P in cloned transfected cells. Rama 37 cells transfected with empty expression vector (Rama 37 + vector control; (**a**–**c**)) or Rama 37 cells overexpressing wild-type S100P (Rama 37 + S100P; (**d**–**f**)), K95A mutant S100P (Rama 37 + S100P K95A; (**g**–**i**)), or ΔK95 mutant S100P (Rama 37 + S100P ΔK95; (**j**–**l**)) were grown on fibronectin-coated coverslips for 48 h prior to fixation, permeabilisation, and staining using secondary antibody coupled to fluorescein isothiocyanate for NMMIIA (**a**,**d**,**g**,**j**) or Cy-3 for S100P (**b**,**e**,**h**,**k**). Cells were then mounted and viewed using a Zeiss LSM510 confocal laser scanning microscope. Merged images (**c**,**f**,**i**,**l**) are shown with overlaps in yellow. Arrows in (**a**,**c**,**g**,**j**) show filamental structures along the edge of the cell. The arrow in (**d**) shows foci of NMMIIA staining near the leading edge of the cell, which did not co-localise with S100P (**f**). The arrows in (**e**,**f**) show a large focus of S100P co-staining with NMMIIA in the perinuclear region. Bars, 10 µm in all panels.

Although cells expressing the S100P mutant proteins (**Figure 1**g–l) exhibited less intense fluorescence than the wild-type protein, they did not exhibit to the same extent the localised foci of S100P or NMMIIA found in cells expressing wild-type

protein. Instead, clear filamental structures of NMMIIA were observed at the cell periphery (**Figure 1**g,j) that resembled those observed in the control S100P-negative cells (**Figure 1**a). The proportion of K95A and ΔK95 mutant-S100P-protein-expressing cells that displayed a NMMIIA filamental structure resembling that of the S100P-negative control cells was not significantly different from the S100P-negative cells (K95A, p = 0.506; ΔK95, p = 0.818). It has been reported that S100P does not bind to NMMIIB [19]. Thus, it might be expected that the presence of S100P would not be associated with altered cytoskeletal arrangement of NMMIIB. The percentage of S100P-negative and S100P-expressing cells that exhibited the NMMIIB filamental structure found predominantly in the S100P-negative control cells was determined. The results showed that for cells expressing wild-type S100P or the K95A or ΔK95 mutant proteins, the percentage of cells expressing the myosin distribution characteristic of the S100P-negative cells was not significantly different from the S100P-negative control cells (p = 0.973, 0.919, and >0.9999, respectively).

In S100P-negative, non-metastatic control cells, vinculin and paxillin were complexed into large foci at the ends of bundled actin filaments. Cells expressing wild-type S100P exhibited a 4.3- or 3.5-fold reduction in the mean number of vinculin- or paxillin-positive focal adhesions per cell, respectively, compared to S100P-negative control cells (**Table 2**; both p < 0.0001). In contrast, cells expressing the K95A mutant S100P protein showed 2.1- and 1.8-fold higher numbers of vinculin and paxillin focal adhesions per cell, respectively, than wild-type S100P cells (vinculin and paxillin, both p < 0.0001) but 48% and 53% of those in the S100P-negative, control cells (**Table 2**; vinculin and paxillin, both p < 0.0001). ΔK95-mutant S100P protein exhibited mean numbers of vinculin and paxillin clusters per cell (**Table 2**) 5.1- and 4.5-fold higher, respectively, than cells expressing wild-type protein (both p < 0.0001) but, surprisingly, also 1.2- and 1.3-fold higher than the control cells (vinculin, p 0.0017; paxillin, p < 0.0001). These results suggest that mutation/deletion of the C-terminal lysine reduces the ability of S100P to alter the cytoskeletal organisation, a possible consequence of the reduced interaction of S100P with NMMIIA.

Table 2. Quantitation of focal adhesions in cell lines with and without metastatic potential.

	Focal Vinculin [a]			Focal Paxillin [a]		
	No of Cells Counted	Mean Focal Adhesions/ Cell ± SD [b]	Mean Focal Adhesions as % of Vector Control	No of Cells Counted	Mean Focal Adhesions/ Cell ± SD [b]	Mean Focal Adhesions as % of Vector Control
Vector control	52	16.8 ± 4.0	100	54	15.2 ± 5.4	100
Wild-type S100P	51	3.9 ± 2.9 *	23.2	53	4.4 ± 3.1 **	28.9
K95A-mutant S100P	52	8.1 ± 4.7 ¶	48.2	51	8.0 ± 4.2 ¶¶	52.6
ΔK95-mutant S100P	51	19.8 ± 6.2 §	117.9	50	20.0 ± 5.2 §§	131.6

[a] *Cloned cell lines were stained for either vinculin or paxillin as described in Materials and Methods. Vinculin or Paxillin-stained focal adhesions were counted in about 50 cells from three independent experiments and the mean and standard deviation (SD) of the number per cell were calculated. b Significance of difference between 2 variables identified was calculated using Mann–Whitney U-test. * Significantly fewer vinculin focal adhesions than S100P-negative vector clone control cells (p < 0.0001). ** Significantly fewer paxillin focal adhesions than S100P-negative vector clone control cells (p < 0.0001). ¶ Significantly more vinculin focal adhesions than cell-clone-expressing wild-type S100P (p < 0.0001) but significantly fewer than S100P-negative vector clone control cells (p < 0.0001) and cell-clone-expressing ΔK95 mutant S100P (p < 0.0001). ¶¶ Significantly more paxillin focal adhesions than cell-clone-expressing wild-type S100P (p < 0.0001) but significantly fewer than S100P-negative vector clone control cells (p < 0.0001) and cell-clone-expressing ΔK95 mutant S100P (p < 0.0001). § Significantly more vinculin focal adhesions than cell-clone-expressing wild-type S100P (p < 0.0001) and significantly more than S100P-negative vector clone control cells (p = 0.0017). §§ Significantly more paxillin focal adhesions than cell-clone-expressing wild-type S100P (p < 0.0001) and significantly more than S100P-negative vector clone control cells (p < 0.0001).*

4. The Effect of S100P Mutants on Transwell and Scratch-Wound Cell Migration

Given their reduction in metastatic potential and the key role of cell migration in metastasis [32], the effect of the C-terminal mutants on S100P-directed cellular migration was tested using two independent assays of cellular motility, Transwell

migration [33], and scratch-wound closure [34][35] (**Figure 2**). In **Figure 2**, results of the Transwell migration assays are expressed as a percentage of the number of untreated, S100P-negative control cells passing through the membrane, whereas the results of the scratch migration assays are expressed as a percentage of the time-to-wound closure of untreated S100P-negative control cells (slower migration rate indicated by a longer time-to-wound-closure). Cells expressing wild-type S100P protein exhibited a 3-fold higher rate of Transwell migration than S100P-negative control cells transfected with empty vector (*p* < 0.0001, **Figure 2**a). In contrast, cells expressing the K95A or ΔK95 mutant S100P proteins exhibited Transwell migration rates that were reduced to 35 and 38%, respectively, of that of cells expressing wild-type S100P protein (K95A and ΔK95 both *p* < 0.0001) and not significantly 1.13- and 1.22-fold higher than S100P-negative, control cells (K95A, *p* = 0.695; ΔK95, *p* = 0.147; **Figure 2**a).
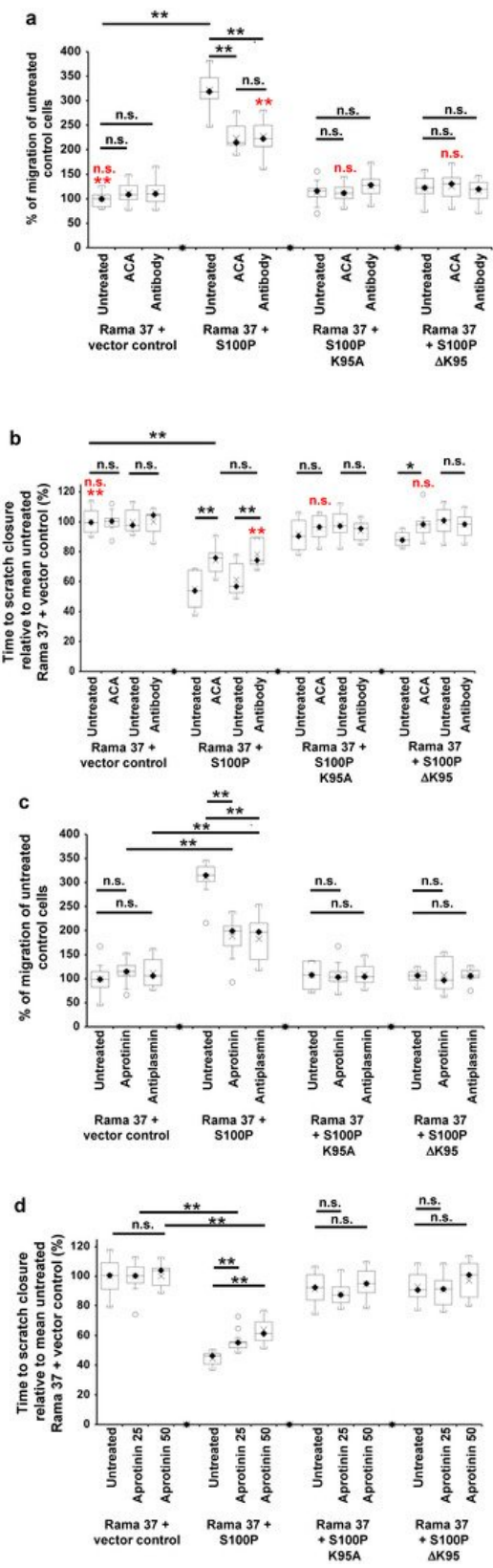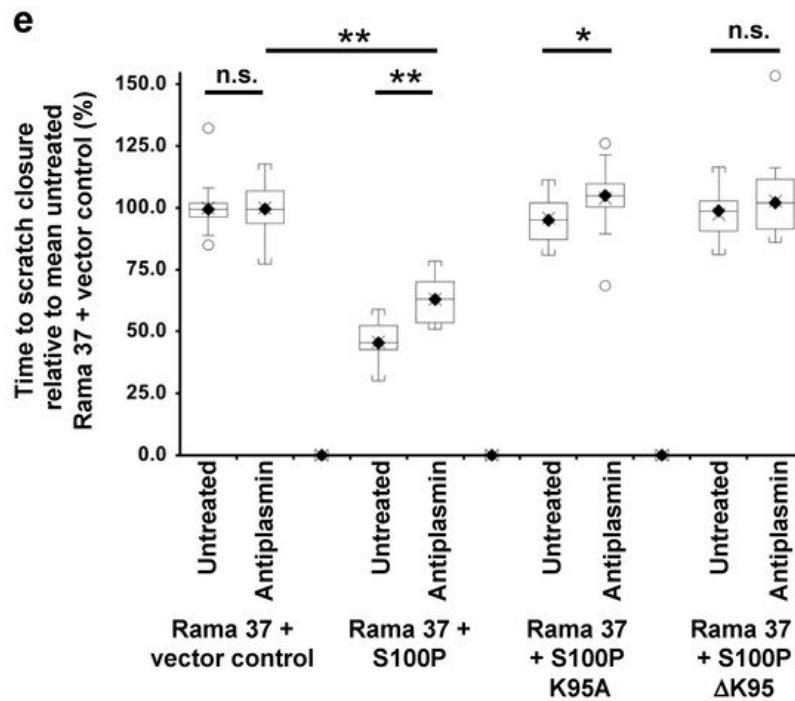
Figure 2. Effect of 6-aminocaproic acid, S100P antibody, aprotinin, or α-2-antiplasmin on migration of cells expressing wild-type and mutant S100P proteins. Transwell migration assays (**a**,**c**) or scratch migration assays in a Cell-IQ incubator (**b**,**d**,**e**) were carried out as described in Materials and Methods for cells expressing wild-type S100P (Rama 37 + S100P), K95A-mutant of S100P (Rama 37 + S100P K95A), ΔK95 mutant of S100P (Rama 37 + S100P ΔK95), or cells not expressing S100P (Rama 37 + vector control). In (**a**,**c**), the number of cells passing through to the underside of the membrane in 16 h were counted and are plotted as percentages of the mean number of untreated Rama 37 + vector control cells passing through the membrane. In (**b**,**d**,**e**), the times to scratch-wound closure are expressed as a percentage of the mean value for untreated Rama 37 + vector control cells. The effect on migration of cells of addition to the extracellular medium (upper and lower chambers in the case of Transwell assays) of 10 mM 6-aminocaproic acid (ACA, panels **a**,**b**) or of an R&D Systems polyclonal goat S100P-specific antibody (Cat No. AF2957) at a concentration of 0.2 ng/µL in the medium (Antibody, panels **a**,**b**) are shown. Each box and whisker plot shows the dispersion of data from 14 (**a**) or 11–12 (**b**) wells in two independent experiments carried out at different times. (**c**) Effect on Transwell migration of 50 µg/mL aprotinin (Aprotinin) or 10 µg/mL α-2-antiplasmin (Antiplasmin) in the extracellular medium. (**d**) Effect on scratch-wound migration of 25 µg/mL aprotinin (Aprotinin 25) or 50 µg/mL aprotinin (Aprotinin 50) in the extracellular medium. (**e**) Effect of 10 µg/mL α-2-antiplasmin (Antiplasmin) on scratch-wound migration. Each box and whisker plot shows the dispersion of data from 14 (**c**) or 14–25 wells (**d**,**e**) in two independent experiments carried out at different times. In all panels, p-values are indicated for comparison between the box and whisker plots beneath the ends of the horizontal lines as not significant (n.s., $p > 0.05$), or significant * (p between 0.001 and 0.05) or ** ($p < 0.0001$). For clarity, some p-value comparisons are shown without lines and in red colour, as follows: (**a**), n.s., Transwell assay Rama 37 + S100P K95A or Rama 37 +ΔK95 in the presence of 6-aminocaproic acid not significantly different from vector control (Dunnett post-hoc multiple comparison with a control); ** Rama 37 +S100P antibody significantly faster than Rama 37 + vector control, $p < 0.0001$; (**b**), scratch-wound assay, n.s. Rama 37 + S100P K95A or Rama 37 + ΔK95 in the presence of 6-aminocaproic acid not significantly different from vector control; ** Rama 37 +S100P antibody significantly faster than Rama 37 + vector control ($p < 0.0001$). In all boxes, the black diamond and line show the median value; the cross shows the mean value. The white circles outside the whiskers denote outliers of >1.5 times the interquartile range.

Since migration rates in Transwell chambers are influenced by serum chemotaxis, directional cellular migration was tested using a scratch-wound assay. The wild-type S100P-expressing cells closed the scratch wound 1.7-fold faster than the S100P-negative control cells ($p < 0.0001$, **Figure 2**b); however, cloned cells expressing the K95A or ΔK95 mutant S100P proteins closed the scratch wound 63% and 62.5%, respectively, slower than cells expressing wild-type S100P (K95A and ΔK95, both $p < 0.0001$; **Figure 2**b just 1.06- and 1.06-fold faster than S100P-negative, control cells (K95A, $p = 0.172$; ΔK95, $p = 0.126$; **Figure 2**b). These results show that the presence of the C-terminal lysine of S100P is associated with the S100P-enhanced cell migration.

References

1. Salama, I.; Malone, P.S.; Mihaimeed, F.; Jones, J.L. A review of the S100 proteins in cancer. Eur. J. Surg. Oncol. 2007, 34, 357–364.

2. Gross, S.R.; Sin, C.G.; Barraclough, R.; Rudland, P.S. Joining S100 proteins and migration: For better or for worse, in sickness and in health. Cell. Mol. Life Sci. CMLS 2014, 71, 1551–1579.

3. Wang, G.; Platt-Higgins, A.; Carroll, J.; de Silva Rudland, S.; Winstanley, J.; Barraclough, R.; Rudland, P.S. Induction of metastasis by S100P in a rat mammary model and its association with poor survival of breast cancer patients. Cancer Res. 2006, 66, 1199–1207.

4. Maciejczyk, A.; Lacko, A.; Ekiert, M.; Jagoda, E.; Wysocka, T.; Matkowski, R.; Halon, A.; Gyorffy, B.; Lage, H.; Surowiak, P. Elevated nuclear S100P expression is associated with poor survival in early breast cancer patients. Histol. Histopathol. 2013, 28, 513–524.

5. Yuan, R.H.; Chang, K.T.; Chen, Y.L.; Hsu, H.C.; Lee, P.H.; Lai, P.L.; Jeng, Y.M. S100P expression is a novel prognostic factor in hepatocellular carcinoma and predicts survival in patients with high tumor stage or early recurrent tumors. PLoS ONE 2013, 8, e65501.

6. Diederichs, S.; Bulk, E.; Steffen, B.; Ji, P.; Tickenbrock, L.; Lang, K.; Zanker, K.S.; Metzger, R.; Schneider, P.M.; Gerke, V.; et al. S100 family members and trypsinogens are predictors of distant metastasis and survival in early-stage non-small cell lung cancer. Cancer Res. 2004, 64, 5564–5569.

7. Shen, Z.Y.; Fang, Y.; Zhen, L.; Zhu, X.J.; Chen, H.; Liu, H.; Jiang, B.; Li, G.X.; Deng, H.J. Analysis of the predictive efficiency of S100P on adverse prognosis and the pathogenesis of S100P-mediated invasion and metastasis of colon adenocarcinoma. Cancer Genet. 2016, 209, 143–153.

8. Wang, Q.; Zhang, Y.N.; Lin, G.L.; Qiu, H.Z.; Wu, B.; Wu, H.Y.; Zhao, Y.; Chen, Y.J.; Lu, C.M. S100P, a potential novel prognostic marker in colorectal cancer. Oncol. Rep. 2012, 28, 303–310.

9. Surowiak, P.; Maciejczyk, A.; Materna, V.; Drag-Zalesinska, M.; Wojnar, A.; Pudelko, M.; Kedzia, W.; Spaczynski, M.; Dietel, M.; Zabel, M.; et al. Unfavourable prognostic significance of S100P expression in ovarian cancers. Histopathology 2007, 51, 125–128.

10. Wang, X.; Tian, T.; Li, X.; Zhao, M.; Lou, Y.; Qian, J.; Liu, Z.; Chen, H.; Cui, Z. High expression of S100P is associated with unfavorable prognosis and tumor progression in patients with epithelial ovarian cancer. Am. J. Cancer Res. 2015, 5, 2409–2421.

11. Zhang, H.; Wang, G.; Ding, Y.; Wang, Z.; Barraclough, R.; Rudland, P.S.; Fernig, D.G.; Rao, Z. The crystal structure at 2Å resolution of the Ca2+ -binding protein S100P. J. Mol. Biol. 2003, 325, 785–794.

12. Lee, Y.C.; Volk, D.E.; Thiviyanathan, V.; Kleerekoper, Q.; Gribenko, A.V.; Zhang, S.; Gorenstein, D.G.; Makhatadze, G.I.; Luxon, B.A. NMR structure of the Apo-S100P protein. J. Biomol. NMR 2004, 29, 399–402.

13. Elliott, P.R.; Irvine, A.F.; Jung, H.S.; Tozawa, K.; Pastok, M.W.; Picone, R.; Badyal, S.K.; Basran, J.; Rudland, P.S.; Barraclough, R.; et al. Asymmetric mode of Ca(2)(+)-S100A4 interaction with nonmuscle myosin IIA generates nanomolar affinity required for filament remodeling. Structure 2012, 20, 654–666.

14. Donato, R. S100: A multigenic family of calcium-modulated proteins of the EF-hand type with intracellular and extracellular functional roles. Int. J. Biochem. Cell. Biol. 2001, 33, 637–668.

15. Penumutchu, S.R.; Chou, R.H.; Yu, C. Structural insights into calcium-bound S100P and the V domain of the RAGE complex. PLoS ONE 2014, 9, e103947.

16. Clarke, C.; Gross, S.R.; Ismail, T.M.; Rudland, P.S.; Al-Medhtiy, M.; Santangeli, M.; Barraclough, R. Activation of tissue plasminogen activator by metastasis-inducing S100P protein. Biochem. J. 2017, 474, 3227–3240.

17. Koltzscher, M.; Neumann, C.; Konig, S.; Gerke, V. Ca2+-dependent binding and activation of dormant ezrin by dimeric S100P. Mol. Biol. Cell 2003, 14, 2372–2384.

18. Heil, A.; Nazmi, A.R.; Koltzscher, M.; Poeter, M.; Austermann, J.; Assard, N.; Baudier, J.; Kaibuchi, K.; Gerke, V. S100P is a novel interaction partner and regulator of IQGAP1. J. Biol. Chem. 2011, 286, 7227–7238.

19. Du, M.; Wang, G.; Ismail, T.M.; Gross, S.; Fernig, D.G.; Barraclough, R.; Rudland, P.S. S100P dissociates myosin IIA filaments and focal adhesion sites to reduce cell adhesion and enhance cell migration. J. Biol. Chem. 2012, 287, 15330–15344.

20. Austermann, J.; Nazmi, A.R.; Muller-Tidow, C.; Gerke, V. Characterization of the Ca2+ -regulated ezrin-S100P interaction and its role in tumor cell migration. J. Biol. Chem. 2008, 283, 29331–29340.

21. Zhang, S.; Wang, G.; Liu, D.; Bao, Z.; Fernig, D.G.; Rudland, P.S.; Barraclough, R. The C-terminal region of S100A4 is important for its metastasis-inducing properties. Oncogene 2005, 24, 4401–4411.

22. Ismail, T.; Fernig, D.; Rudland, P.; Terry, C.; Wang, G.; Barraclough, R. The basic C-terminal amino acids of calcium-binding protein S100A4 promote metastasis. Carcinogenesis 2008, 29, 2259–2266.

23. Davies, B.R.; Davies, M.P.A.; Gibbs, F.E.M.; Barraclough, R.; Rudland, P.S. Induction of the metastatic phenotype by transfection of a benign rat mammary epithelial cell line with the gene for p9Ka, a rat calcium-binding protein but not with the oncogene EJ ras-1. Oncogene 1993, 8, 999–1008.

24. Oates, A.J.; Barraclough, R.; Rudland, P.S. The identification of osteopontin as a metastasis-related gene product in a rodent mammary tumour model. Oncogene 1996, 13, 97–104.

25. Liu, D.; Rudland, P.S.; Sibson, D.R.; Platt-Higgins, A.; Barraclough, R. Human homologue of cement gland protein, a novel metastasis inducer associated with breast carcinomas. Cancer Res. 2005, 65, 3796–3805.

26. Lloyd, B.H.; Platt-Higgins, A.; Rudland, P.S.; Barraclough, R. Human S100A4 (p9Ka) induces the metastatic phenotype upon benign tumour cells. Oncogene 1998, 17, 465–473.

27. El-Tanani, M.K.; Barraclough, R.; Wilkinson, M.C.; Rudland, P.S. Regulatory region of metastasis-inducing DNA is the binding site for T cell factor-4. Oncogene 2001, 20, 1793–1797.

28. Rudland, P.S.; Platt-Higgins, A.; Renshaw, C.; West, C.R.; Winstanley, J.H.R.; Robertson, L.; Barraclough, R. Prognostic significance of the metastasis-inducing protein S100A4 (p9Ka) in human breast cancer. Cancer Res. 2000, 60, 1595–1603.

29. Rudland, P.S.; Platt-Higgins, A.; El-Tanani, M.; De Silva Rudland, S.; Barraclough, R.; Winstanley, J.H.R.; Howitt, R.; West, C.R. Prognostic significance of the metastasis-associated protein osteopontin in human breast cancer. Cancer Res. 2002, 62, 3417–3427.

30. Barraclough, D.L.; Platt-Higgins, A.; de Silva Rudland, S.; Barraclough, R.; Winstanley, J.; West, C.R.; Rudland, P.S. The metastasis-associated anterior gradient 2 protein is correlated with poor survival of breast cancer patients. Am. J. Pathol. 2009, 175, 1848–1857.

31. Ismail, T.M.; Zhang, S.; Fernig, D.G.; Gross, S.; Martin-Fernandez, M.L.; See, V.; Tozawa, K.; Tynan, C.J.; Wang, G.; Wilkinson, M.C.; et al. Self-association of calcium-binding protein S100A4 and metastasis. J. Biol. Chem. 2010, 285, 914–922.

32. Jenkinson, S.R.; Barraclough, R.; West, C.R.; Rudland, P.S. S100A4 regulates cell motility and invasion in an in vitro model for breast cancer metastasis. Br. J. Cancer 2004, 90, 253–262.

33. Chen, H.C. Boyden chamber assay. Methods Mol. Biol. 2005, 294, 15–22.

34. Cory, G. Scratch-wound assay. Methods Mol. Biol. 2011, 769, 25–30.

35. Liang, C.C.; Park, A.Y.; Guan, J.L. In vitro scratch assay: A convenient and inexpensive method for analysis of cell migration in vitro. Nat. Protoc. 2007, 2, 329–333.